2012 2nd International Conference on Environment and Industrial Innovation
IPCBEE vol.35 (2012) © (2012) IACSIT Press, Singapore

Heat Transfer from An Impingement Jet onto A Heated Half-Prolate Spheroid Attached to A Heated Flat Plate

Patricia Streufert and Terry X. Yan [+]

Department of Mechanical and Industrial Engineering
Southern Illinois University Edwardsville
Edwardsville, IL 62026 USA

Abstract. Impingement jet heat transfer behavior is numerically investigated for a target surface consisting of a half-prolate spheroid attached to a flat plate. The Reynolds-averaged Navier-Stokes equations (RANS) and the energy equation are solved for axisymmetric, three-dimensional flow. The k-ε rng and v2f turbulence models with non-uniform meshes are used for the simulations. One jet-to-target distance is used and five spheroid shapes are investigated for a Reynolds number of 23,000. A number of effects are studied for each model including location of separation point, local heat transfer and stagnation point Nusselt number. Existing experimental data for a half-round dome (a/c = 1) is used to compare with these numerical results.

Keyword: impinging jet, heat transfer

1. Introduction

Jet impingement has been used in a wide variety of industrial heating and cooling applications[1]. Impingement jets are used, for example, to cool hot gas turbine blades, dry paper, to de-ice aircraft wings in severe weather, and to cool sensitive electronic equipment. Thus the application of this technology is widespread and diverse and understanding the behavior of various geometries is of great interest.

There is a vast amount of literature on the study of impinging jet fluid flow and heat transfer (Gardon and Akfirat [2], Martin [3]), but very little literature addressing the issue in this study – jet impingement onto a curved surface, most of it experimental rather than computational. Computational fluid dynamic simulations are extensively used in design analysis, as well as in academic studies (Craft *et al.* [4]), and are of great value in determining various parameter effects such as nozzle-to-plate distance or jet exit profile shape, or in this case, the shape of the elliptical dome that is impinged upon by the circular air jet.

Very little of the research has been done to date on the effect of a curved surface on the heat transfer rate of an impingement jet, both using convex and concave target zones. Saniei and Yan [5], conducted experiments to measure the heat transfer for a heated hemispherical dome attached to a base plate, subjected to a circular air impingement jet. They found that the heat transfer behaviors of the circular dome to be similar to those for a flat plate. Lee *et al* [6], experimentally studied the heat transfer effects from a circular air-jet impinging on a convex surface at Re = 11,000, 23,000, and 50,000. They found that maximum stagnation Nusselt number occurs at L/D = 6~8, which they found was where the jet turbulent intensity reaches a maximum value in the stagnation region. More importantly, they found that the Nusselt numbers for both the stagnation point region and wall jet region increase with increasing surface curvature.

Lim *et al* [7] measured the local heat transfer coefficients on a hemispherical convex surface with a round air-impinging jet, studying the effects of inclination of the jet to the surface at Re = 23,000. They

[+] Corresponding author. Tel.: 618-650-3463 ; fax: 618-650-2555.
E-mail address: xyan@siue.edu.

showed that at zero angle (perpendicular to the surface) the stagnation Nusselt number is relatively impervious to jet-to-surface (L/D) distance, but that the secondary maximum observed in flat plate measurements also exists on a convex surface at lower L/D distances.

Hu and Zhang [8] conducted a series of experimental and numerical studies on a circular water jet impinging on a convex hemispherical surface. They studied jet Reynolds numbers from Re = 1947 – 19,478, with nozzle-to-surface distances of L/D = 2.5 – 25. They assumed laminar flow in their modeling and found that the Nusselt number at stagnation was higher for a convex surface than for a flat surface with equal L/D, with their numerical results agreeing well with their experimental results at stagnation.

Rahman and Hernandez [9], analyzed the heat transfer from a heated convex surface to a water impingement jet at low Reynolds numbers, Re = 500-1500. They investigated different materials and differing thicknesses of the convex surface, and found the largest heat flux at the stagnation region, and that a material with lower thermal conductivity gives higher average Nusselt number.

The V2F turbulence model developed by Durbin [10, 11] and Behnia *et al.* [13] was used in calculating the turbulent kinematic viscosity for the computational model. The comparison of the standard k-ε model and the V2F model shows clearly that the V2F model matched test data trends better than the standard k-ε model and was in good agreement with the experimental results of Yan [12].

The objective of the present research is to evaluate the effect of ellipticity on the heat transfer from a curved surface to an air impingement jet. Five levels of ellipticity were investigated from a round dome, with ellipticity e = 1.0, to four curved shapes with varying degrees of ellipticity (e = 0.75, 0.5, 0.33, and 0.25).

The Reynolds number was fixed at Re = 23,000, for the various degrees of elliptic. The equatorial radius, a, is kept constant for each ellipse with only the polar radius, b, changing for each degree of ellipticity. The jet-to-plate distance is kept constant at L/D = 4.

2. Problem Description

2.1. Objective

A Newtonian fluid (air, Pr = 0.71) exits a pipe with a specified velocity profile, and impinges on a prolate spheroid attached to a flat plate whose plane is at 90° to the axis of the jet. The flow is steady and incompressible. The jet temperature is set at 300 K, the same as the temperature of ambient stagnant air.

Spheroids with differing degrees of ellipticity were studied. The ellipticity is defined as the polar radius, b, of the ellipse, divided by the equatorial radius, a, such that a smaller degree of ellipticity translates to a "pointier" shape. The polar radius, b, varied with each degree of ellipticity while the equatorial radius, a, was kept constant at 8.89 cm to match the experimental setup of Saniei and Yan [5]. Figure 2 illustrates the various ellipticities studied: e = 1.0, 0.75, 0.5, 0.33, and 0.25.

2.2. Coordinates and Computational Domain

The computational domain shown in Figure 3 was chosen to simulate the experimental conditions of Seniai and Yan [5]. The domain on *r* axis is taken as 10 times the impingement jet diameter. The Reynolds number is based on the jet diameter and was set at 23,000, 14,000, 10,000, and 5,000. A velocity profile was defined directly at the jet exit based on a previous study by Yan and Streufert [14]. The impingement dome and plate were modeled as non- slip walls, with a constant heat flux of 500 W/m^2. The inlet pipe wall is modeled as an adiabatic wall with a no slip boundary condition. A pressure outlet boundary condition is used at the outlet. The gauge pressure was set as zero, which implies that at the outlet the pressure is at the atmospheric pressure. As the outlet is far away from the jet, a back flow temperature was set as 300 K. A pressure inlet condition was set at the top of the domain to include the effect of entrainment. The backflow temperature was set as 300 K. The fluid properties are specified as those of air at STP.

2.3. Governing Equations

The governing equations for the time-averaged, turbulent, steady, single phase, incompressible and three-dimensional flow are the standard equation set[14]

2.4. Turbulence Modeling

The Bousinessq eddy viscosity concept applied to the Reynolds stress as

$$-\rho\overline{u_i'u_j'} = \mu\left(\frac{\partial u_i}{\partial x_j} + \frac{\partial u_j}{\partial x_i}\right) - \frac{2}{3}\rho k\delta_{ij} \tag{1}$$

where k is turbulent (fluctuating motion) kinetic energy. Turbulent transport of energy and other scalar variables are modeled in a similar way. By analogy to equation (4), the turbulent transport of a scalar is taken to be proportional to the gradient of the mean value of the transported quantity:

$$-\rho\overline{u_j'\phi'} = \Gamma_t \frac{\partial \phi}{\partial x_j} \tag{2}$$

where Γ_t is the turbulent diffusivity (μ_t/Pr_t), ϕ is a scalar variable and Pr_t is the turbulent Prandtl number. The turbulence model uses additional transport equations to solve for μ_t and Γ_t that appears in equations 4 and 5 respectively. The number of additional equations solved depends on the turbulence model chosen.

The RNG k-ε turbulence model [15], differs from the standard k-ε model in a few aspects. The RNG model solves an additional term in the ε equation compared to the standard k-ε model, and it solves an analytical formula for turbulent Prandtl numbers. The standard k-ε model on the other hand uses user-specified, constant values. The RNG model also provides for an option to treat the effective viscosity using the analytically derived formula that accounts for low-Reynolds-number effect .

TheV2F model is a four-equation turbulence model developed by Durbin [10, 11]. It solves two additional equations in comparison to the k-ε model: a velocity variance scale ($\overline{v^2}$) and an elliptic relaxation factor (f). This model was developed with an aim to improve the effects of the walls on the turbulence. The presence of the wall affects the fluctuations in the wall-normal stress $\overline{v^2}$ in two ways. The wall damping of $\overline{v^2}$ is felt by the turbulence fairly far from the wall ($y^+ \leq 200$) through the pressure field, whereas the viscous damping takes place within the viscous and buffer layer ($y^+ \leq 20$). In usual eddy-viscosity models, both these effects are accounted for through damping functions, whereas the damping of $\overline{v^2}$ in the RSM model is accounted through the modeled pressure-strain terms. In the V2F model the problem of accounting for the wall damping of $\overline{v^2}$ is simply resolved by solving the transport equation of $\overline{v^2}$.

The turbulence kinetic energy, k, its rate of dissipation, ε, the velocity variance scale, $\overline{v^2}$, and the elliptic relaxation function, f, are obtained from the 4 transport equations[11, 13]. The eddy-viscosity (μ_t) is modeled using one time scale (T) and one velocity scale ($\overline{v^2}$) instead of the turbulence kinetic energy (k) used in the k-ε model. The velocity variance scale $\overline{v^2}$ (can be thought of as the velocity fluctuations normal to the streamlines). This distinguishing feature of the V2F model seems to provide a proper scaling in representing the damping of turbulent transport close to the wall, a feature that k does not provide in other eddy-viscosity model

$$\mu_t = \rho C_\mu \overline{v^2} T \tag{3}$$

2.5. Numerical Scheme

A finite volume method code was used in this research to solve the governing equations. A non-uniform grid system is used in both r-direction and x-direction. Finer grids near the wall and close to the jet center axis are obtained. Nodes are concentrated in the regions of high gradients, i.e. the impinging wall and shear layer. For the V2F model, the wall y^+ value on the impinging wall is maintained near 1.0 in order to satisfy the requirements of the turbulence models.

3. Results and discussion

A typical flow field for domes with five different ellipticity is shown in Figure 3. The Reynolds numbers are all for Re= 46,000. The ellipticity decreases as the dome changes from a hemisphere to a pointed ellipse (from left to right). The flow streamline on the surface began to lift off the surface, signaling a flow

separation at a large arch length close to the flat base plate. The separation is further delayed as the dome becomes more ellipical.

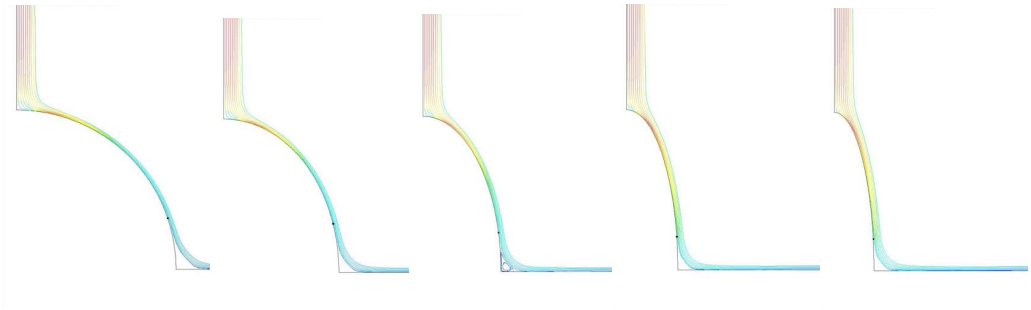

Figure 3 Flow Contours

3.1. Effect of Ellipticity on Heat Transfer

The predicted heat transfer on the hemispheric dome (e=1) for a Reynolds number of 23,000 is compared with the experimental results of Sanie and Yan [5] for the same conditions in Figure 4. The predicted stagnation point heat transfer is 12 % higher. This trend was observed in the stagnation heat transfer prediction for a flat plate with different jet flow profiles [14]. This could be due to the poor prediction ability of the turbulence modes used at the stagnation region where largest flow strain rate is experienced by the flow as the flow transit from stagnation to a wall boundary layer type of flow. At the S/D of about 2 the prediction matches well with the experiments. As the S/D increases for the boundary layer flow, the predicted heat transfer decreases along the surface till it reaches the separation points at around S/D ~ 5.75. After the flow transition from flow along a curvature to a straight surface, the predicted heat transfer follow the pattern of a flat plate boundary flow, but with a consistent over prediction of about 10-15 %. The general assessment of the numerical model is fair to good, given the fact that impinging jet is one of the flow cases that offers challenges to turbulence models ([4], [10]).

Figures 5 (a) and 5(b) show the heat transfer distribution along the domes and the flat base section for five ellipticities for a fixed Reynolds number of 23,000. Figure 5(a) show the raw data with different dome surface lengths, while Figure 5(b) is normalized by the dome arch length up to the dome-to-flat-plate intersection. At the stagnation region, the sharper the dome gets the higher stagnation heat transfer. Away from the stagnation region at about S/D ~ 2, heat transfer data are very close in values, showing a similar flow pattern to begin at the vicinity, a starting a boundary layer flows. The heat transfer in this boundary layer flow region for the two ellipicities, e = 0.25 and 0.33(highest surface curvatures) are higher than those with smaller curvatures (larger elliticities). The flow pattern along the flat-plate section is clearly affected by the upstream flow conditions, with a higher local heat transfer for the smallest ellipicity, (e=0.25). As we see from Figure 3, the more pointed a dome gets the later the flow separation occurs on the dome surface, thus allowing more momentum in the flow to contribute to the heat transfer process down stream on the flat plate. As seen in Figure 5(a) the flat-plate sections in the domain have different lengths, with the hemispherical dome having the minimum flat-plate section. The heat transfers at the tail-end of the flat plate section approach to the value of the long plate value for all cases.

3.2. Stagnation Point Heat Transfer & Average Heat Transfer

A different view of the heat transfer on a dome surface with a flat-plate base is presented in terms of the stagnation heat transfer in comparison with the average heat transfer on the dome and on the dome-flat-plate combine, Figure 6. As the dome becomes more pointed, i.e. ellipticity *e* becomes smaller, the stagnation point heat transfer becomes larger, while the average heat transfer on the dome surface does not change after *e* = 0.5 (the solid line). The overall average heat transfer maintains a small range of variation, 0.93 to 0.98. The offers some practical guidance in design a cooling scheme for such dome and plate combine geometries.

4. Conclusions

Numerical study to evaluate the effect of ellipticity on the heat transfer from a curved surface to an air impingement jet has carried out in this research. Five levels of ellipticity, *e* (1, 0.75, 0.5, 0.33, and 0.25)

and three Reynolds numbers (Re = 23,000, 14000, 10,000 and 5,000) were used parametrically. The conclusions are drawn as follows:

- Heat transfer distributions on the curve surface of a dome were obtained numerically by utilizing two-equation eddy viscosity turbulence models. They compared with experiments results from fair to good.
- Curve surface flow pattern indicative of flow separation were shown. The separation progresses further downstream as ellipticity decreases.
- Ellipticity has a strong effect on heat transfer, especially at stagnation region. The more pointed a dome becomes (smaller ellipticity), the higher heat transfer in the stagnation region.
- The scaled stagnation point heat transfer is sensitive to ellipticity for the whole range of *e* studied, while the average heat transfer on the dome is less sensitive to ellipticity at the range of $e \geq 0.5$. The overall heat transfer of dome surface and base flat plate combine is not sensitive to ellipticity in the whole range of *e* studied.

5. References

[1] Bergles, A. E., 1997, "Heat Transfer Enhancement - The Encouragement and Accommodation of High Heat Fluxes, " *Journal of Heat Transfer*, Vol. 119, pp. 8-19.

[2] Gardon, R., and Akfirat, J.C., 1965, "The Role of Turbulence in Determining the Heat-Transfer Characteristics of Impinging Jets," International Journal of Heat Mass Transfer, Vol. 8s, pp. 1261-1272.

[3] Martin, H. 1977, "Heat and Mass Transfer between Impinging Gas Jets and Solid Surfaces," Advance in Heat Transfer, Vol. 13, pp.1-60.

[4] Craft, T.J., Graham, L.J.W., and Launder, B.E., 1993, "Impinging Jet Studies for Turbulence Model Assessment – II. An Examination of the Performance of Four Turbulence Models," International Journal of Heat and Mass Transfer, Vol. 36, pp. 2685-2697.

[5] Saniei, N., Yan, X., 1997, "Impingement Cooling of a Hemispherical Dome Attached to a Flat Wall," 1997 National Heat Transfer Conference, Baltimore, MD.

[6] Lee, D.H., Chung, Y.S., Won, S.Y., 1998, "The effect of concave surface curvature on heat transfer from a fully developed round impinging jet," International Journal of Heat and Mass Transfer, Vol. 24, pp 2489-2497.

[7] Lim, K.B., Lee, C.H., Sung, N.W., Lee, S.H., 2006, "An experimental study on the characteristics of heat transfer on the turbulent round impinging jet according to the inclined angle of convex surface using the liquid crystal transient method," Journal of Experimental Thermal and Fluid Science, Vol. 31, pp 711-719.

[8] Hu, G., Zhang, L., 2007, "Experimental and Numerical Study on Heat Transfer with Impinging Circular Jet on a Convex Hemispherical Surface," Journal of Heat Transfer and Engineering, Vol. 28(12), pp 1008-1016.

[9] Rahman, M.M., Hernandez, C.F., 2010, "Transient conjugate heat transfer from a hemispherical plate during free liquid jet impingement on the convex surface," Journal of Heat and Mass Transfer, Vol. 47, pp 69-80.

[10] Behnia, M., Parneix, S., and Durbin, P.A., 1998, "Prediction of Heat Transfer in an Axisymmetric Turbulent Jet Impinging on a Flat Plate," International Journal Heat and Mass Transfer, Vol. 41, pp. 1845-1855.

[11] Durbin, P.A., 1991, "Near-Wall Turbulence Closure without Damping Functions," Theoretical and Computational Fluid Dynamics, Vol. 3, No.1, pp.1-13.

[12] Yan, X., 1993, "A Preheated-Wall Transient Method Using Liquid Crystals for the Measurement of Heat Transfer on External Surfaces and in Ducts," Ph.D. Dissertations, University of California, Davis.

[13] Behnia, M., Parneix, S., Shabany, Y., and Durbin, P.A., 1999, "Numerical Study of Turbulent Heat Transfer in Confined and Unconfined Impinging Jets," International Journal of Heat and Fluid Flow 20,pp. 1-9.

[14] Yan, T. X., Streufert, P., 2010, "Jet Inlet Condition Effect on the Heat Transfer from a Circular Impinging Air Jet to a Flat Plate," Proceedings of the 2010 ASME International Mechanical Engineering Congress, IMECE2010-4079.

[15] Yak hot, V., and Orzag, S.A., 1986, "Renormalization Group Analysis of Turbulence. I. Basics Theory," Journal of Sci. Comp., Vol.1, pp3-51.

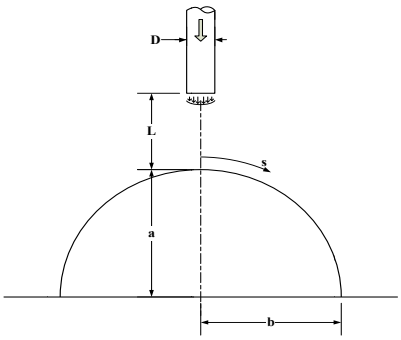

Figure 1(a) – Basic Geometry of Study

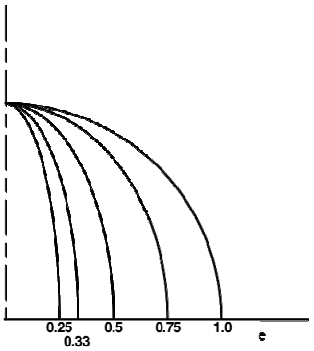

Figure 1 (b) – Ellipticity, e, of each dome

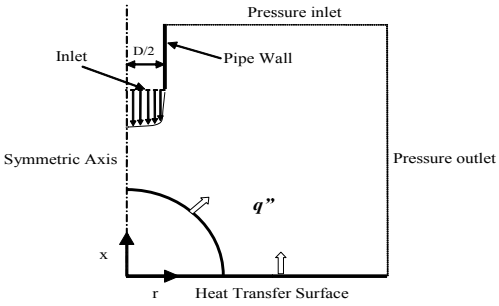

Figure 2 Computational Domain

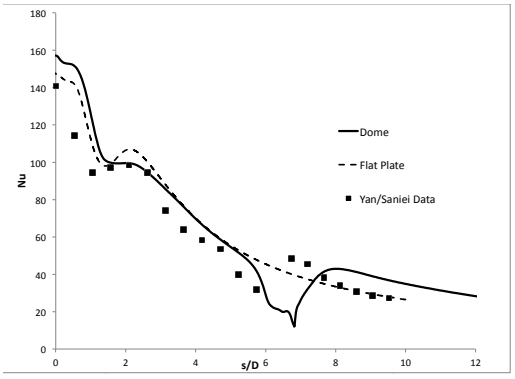

Figure 4 Comparisons with Experimental data

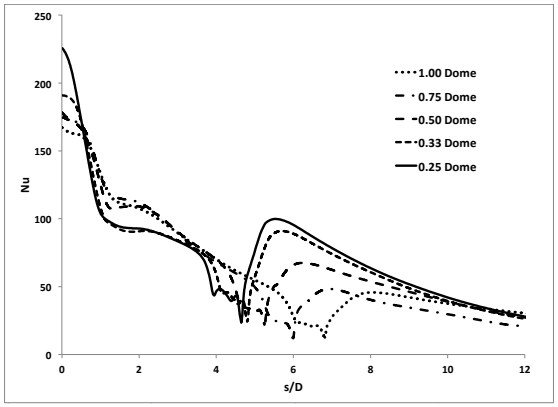

Figure 5(a) Heat Transfer distribution

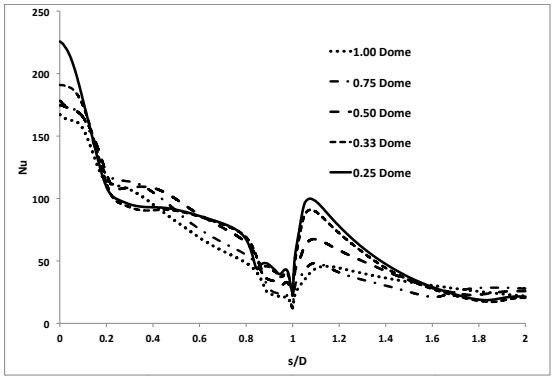

Figure 5(b) normalized heat transfer distribution

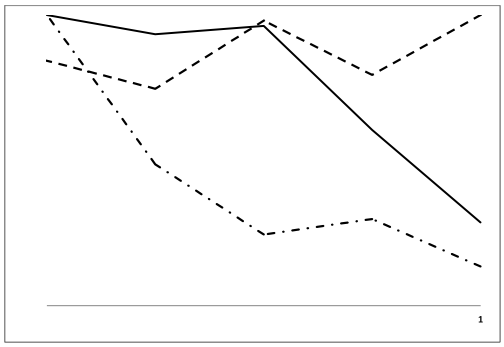

Figure 6 Stagnation point heat transfer